

Article

Chance-Constrained Optimal Design of PV-Based Microgrids under Grid Blackout Uncertainties

Mansour Alramlawi ¹ and Pu Li ^{2,*} 

¹ Department of Cognitive Energy Systems, Fraunhofer IOSB-AST, 98693 Ilmenau, Germany; mansour.alramlawi@iosb-ast.fraunhofer.de

² Department of Process Optimization, Institute of Automation and Systems Engineering, Ilmenau University of Technology, 98693 Ilmenau, Germany

* Correspondence: pu.li@tu-ilmenau.de

Abstract: A grid blackout is an intractable problem with serious economic consequences in many developing countries. Although it has been proven that microgrids (MGs) are capable of solving this problem, the uncertainties regarding when and for how long blackouts occur lead to extreme difficulties in the design and operation of the related MGs. This paper addresses the optimal design problem of the MGs considering the uncertainties of the blackout starting time and duration utilizing the kernel density estimator method. Additionally, uncertainties in solar irradiance and ambient temperature are also considered. For that, chance-constrained optimization is employed to design residential and industrial PV-based MGs. The proposed approach aims to minimize the expected value of the levelized cost of energy (LCOE), where the restriction of the annual total loss of power supply (TLPS) is addressed as a chance constraint. The results show that blackout uncertainties have a considerable effect on calculating the size of the MG's components, especially the battery bank size. Additionally, it is proven that considering the uncertainties of the input parameters leads to an accurate estimation for the LCOE and increases the MG reliability level.

Keywords: microgrid; battery lifetime; optimal design; blackout



Citation: Alramlawi, M.; Li, P.

Chance-Constrained Optimal Design of PV-Based Microgrids under Grid Blackout Uncertainties. *Energies* **2024**, *17*, 1892. <https://doi.org/10.3390/en17081892>

Academic Editor: Anastasios Dounis

Received: 29 February 2024

Revised: 9 April 2024

Accepted: 12 April 2024

Published: 16 April 2024



Copyright: © 2024 by the authors. Licensee MDPI, Basel, Switzerland. This article is an open access article distributed under the terms and conditions of the Creative Commons Attribution (CC BY) license (<https://creativecommons.org/licenses/by/4.0/>).

1. Introduction

MG design is a long-term planning process. In this process, the optimal size and types of the MG components should be selected in such a way that guarantees a long-term reliable and cost-effective energy source based on the customer's requirements. The optimal design of the MG includes a deep understanding of the operation, lifetime characteristics, and environmental impacts of each component in the MG that highly increases the problem complexity. Moreover, considering the uncertainty of fluctuating renewable energy sources and grid blackouts plays an essential role in increasing the optimal design accuracy.

One can classify the solution approach for the optimal design problem of the MG into the following two main categories: (1) deterministic optimal design of MGs and (2) stochastic optimal design of MGs. The former can calculate the optimal sizes of the MG components, but the solution may not be accurate enough to satisfy the design constraints. The latter provides an optimal solution while satisfying the related technical constraints considering the load, electricity cost, or power sources uncertainties. The latter solution approach is the subject of interest in this paper.

Several studies have been conducted to incorporate the uncertainty of renewable power generation in the MG optimal design problem considering different stochastic parameters and models as well as solutions strategies [1,2]. For instance, a chance-constrained programming approach was utilized in [3] to design a standalone wind-PV-battery system considering the non-Gaussian stochastic model for the produced power by the wind turbine and the PV system. In [4], a Monte Carlo simulation (MCS) and practical swarm algorithm were used to find the optimal size of a wind-PV-battery system while considering the

wind speed, solar irradiance, and load demand uncertainty. Also, the optimal size of a PV–wind–battery system was investigated in [5]; meanwhile, MCS was utilized to handle the uncertainty of the wind and the PV system production without considering the seasonal variation in the developed stochastic model. A concept of design space was applied in [6] to optimize the size of a PV–battery system incorporating the uncertainty of the generated power from the PV array, taking into consideration the desired confidence level. Besides, the design space approach was used in [7] for sizing an islanded wind–battery system by considering the wind speed uncertainty. Chance-constrained programming method was used in [8] to address the uncertainties in renewable resources to optimize a PV–wind–battery system. Recently, a scenario reduction method has been proposed to simplify the impact of the uncertainty in the load profile and the renewable energy output on the MG optimal design problem [9].

Special attention was given to optimizing the energy storage system in order to increase MG reliability and decrease the impact of uncertainty. As an example, the work in [10] used the Markov chain method with MCS to calculate the optimal size of the energy storage system in a MG to minimize the power mismatch between the generated power from the renewables and load considering wind speed uncertainty. Moreover, a stochastic optimization problem was formulated in [11] to find the optimal size of a battery storage system in an islanded MG considering the wind speed and the load growth factor uncertainty. In [12], the stochastic optimization problem was transformed into a deterministic one using the point estimated method with Cholesky decomposition to optimize the energy storage size considering the intermittent power generation from the wind turbines. In [13], a stochastic programming technique was used to optimize energy storage system size in a grid-connected MG to enhance its reliability under wind speed uncertainties. Chance-constrained optimization (CCOPT) for optimal power flow was introduced by Zhang and Li [14] and solved efficiently with sparse-grid integration [15]. From the above discussion, it can be noticed that most of the previous studies take into account the uncertainty of the generated power from renewable energy sources and the power consumption by the load. Nevertheless, the impact of grid blackout uncertainty in the MG optimal design problem was considered in very few studies. Although, the grid blackout problem is still present in many countries throughout the world [16–20], and causes a significant economic loss for the customers [21,22]. For instance, in [23], the battery and the diesel generator sizing problem was investigated considering the uncertainty of renewable energy outputs and grid blackouts; however, a simplified stochastic model with linear objective function and constraints were used to formulate the optimization problem. Recently, a simulation-based design method for the battery in a grid-connected PV–battery system for emergence usage was introduced in [24] considering only the yearly grid blackout uncertainty. Besides, in [25] the influence of battery price and customer damage cost on the optimal size of a PV–battery system was explored considering the number of yearly blackouts and its duration uncertainty. It is worth mentioning that parametric probability density functions were used to describe the uncertainty of grid blackout in the studies mentioned previously.

In this paper, a comprehensive method for the optimal design of PV-based MGs, considering the uncertainty of solar radiation, ambient temperature, and grid blackouts is presented. Moreover, for appropriate consideration of the load consumption variation, the deviation in the load consumption on workdays and weekends as well as the seasonal variation in the load profiles are considered. The proposed method aims to minimize the *LCOE* taking into consideration the limitation of the *TLPS* and the MG operational constraints. In addition, a detailed model for battery lifetime estimation is introduced based on the physicochemical mechanism of the lead–acid battery. In comparison to our previous work [26] and the above studies, the major contributions of this study include the following:

- A new model is implemented to model the uncertainty of grid blackout starting time and blackout period using kernel density distribution;
- A novel optimal design method utilizing a chance-constrained approach is developed to optimize the sizes of the MG components considering the uncertainties of solar radiation, ambient temperature, and grid blackout;
- An improved method to calculate the *LOCE* utilizing an accurate estimation of the number of lead–acid battery replacements during the MG lifetime by considering the impact of battery state of charge, discharging current, number of cycles, acid stratification, and sulfate crystal structure on the battery lifetime.

The paper is constructed as follows: Section 2 describes the modeling of the uncertain parameters considered in the optimal MG design. Section 3 presents the formulation of the chance-constrained optimization problem. A numerical solution method to the problem is presented in Section 4. The computation results of case studies are given in Section 5. The paper is concluded in Section 6.

2. Modeling the Uncertain Parameters

In general, there are two methods to model the uncertainties of random parameters using a probability density function (PDF), namely, the parametric and the non-parametric techniques [27]. A parametric PDF involves a standard distribution function, e.g., Gaussian, Beta, and Binomial etc., while a non-parametric PDF is used in the case that a parametric distribution cannot characterize the stochastic behavior of the data accurately.

2.1. Blackouts Uncertainty Model

A grid-tie line status parameter α_g is used to describe the grid performance, as shown in Figure 1. In the event of a grid blackout $\alpha_g = 0$; otherwise $\alpha_g = 1$, which can be expressed as follows:

$$\alpha_g(Bl_{st}, Bl_{pr}) = \begin{cases} 0, & Bl_{st} \leq t \leq Bl_{st} + Bl_{pr} \\ 1, & otherwise, \end{cases} \quad (1)$$

where Bl_{st} and Bl_{pr} are the blackout starting time and the blackout period, respectively, which are uncertain parameters considered in this study. However, it is hard to find a general parametric PDF that describes the uncertainty of such blackout parameters. Therefore, the method of kernel density estimator (KDE) is used in this study to estimate the uncertainty of Bl_{st} and Bl_{pr} . KDE or Parzen's window is a non-parametric density estimator that can formulate its shape from the data itself [28]. A KDE builds for similar data and samples their own probability density curve; then, these curves are smoothed and combined in one curve that represents the PDF for all samples [29,30].

The general formula of a kernel density estimator f_k for any real values of x is given by [28]

$$f_k(x) = \frac{1}{nh} \sum_{i=1}^n K\left(\frac{x - X_i}{h}\right), \quad (2)$$

where n is the samples number, h denotes the bandwidth that controls the smoothness of the KDE probability density curve, K is a smooth function called the kernel function [28], X_1, X_2, \dots, X_n are the random samples. The value of the bandwidth is important to shape the KDE. Choosing a high value for the bandwidth leads to a smooth KDE that may hide some characteristics of the distribution. Meanwhile, a small bandwidth value may overestimate some characteristics of the distribution. In this study, the *ksdensity* function in MATLAB [31] is utilized to generate a PDF of the blackout starting time and blackout period. In *ksdensity*, the optimal value of the bandwidth is calculated based on the method proposed in [29].

As a result, the PDFs of the blackout starting time and the blackout period are determined by the following steps: (1) record the daily status of the grid-tie line (in this study, we use recorded data from an area suffering from long periods of daily blackouts [32]);

(2) extract daily blackout starting time and blackout period; (3) calculate their PDF using the KDE method.

As a result, samples of daily blackout starting time and blackout period (BL_{st}, BL_{pr}) can be generated by using the Cartesian product from the obtained PDE.

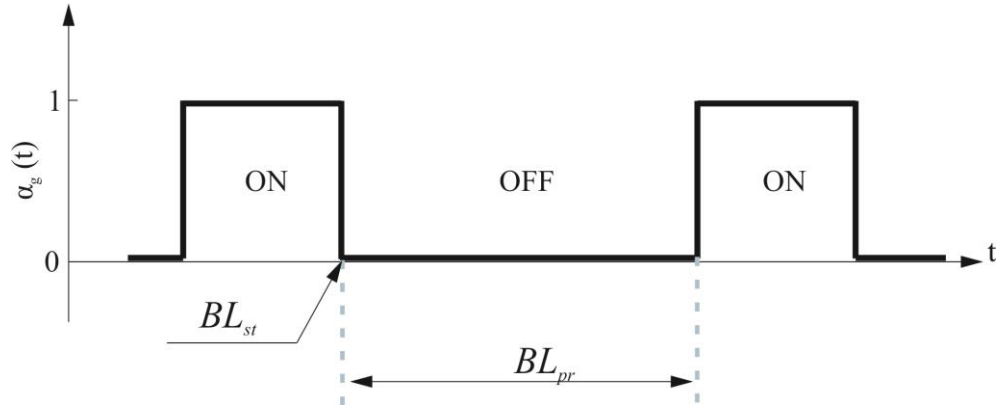


Figure 1. Illustration of the grid-tie line status variable α_g .

2.2. Solar Irradiance Uncertainty Model

The uncertainty of solar irradiance has seasonal and diurnal patterns [33]. It is shown in [34] that solar irradiance uncertainty can be properly described by a Beta PDF [34]:

$$f_G = \frac{\Gamma(\psi + \varrho)}{\Gamma(\psi)\Gamma(\varrho)} G_x^{(\varrho-1)} (1 - G_x)^{(\psi-1)}, \text{ for } \psi \geq 0, \varrho \geq 0, \tag{3}$$

where G_x is the solar irradiance and x refers to the irradiance type that can be global, direct, or diffused. ψ and ϱ are the parameters that can be calculated from the mean value μ and the standard deviation σ of the historical data as [35]

$$\psi = (1 - \mu) \left(\frac{\mu(1 + \mu)}{\sigma^2} - 1 \right), \tag{4}$$

$$\varrho = \frac{\psi\mu}{(1 - \mu)}. \tag{5}$$

In this study, an hourly Beta-PDF for the solar irradiance at each hour is used (see Figure 2) where the seasonal variation is also considered.

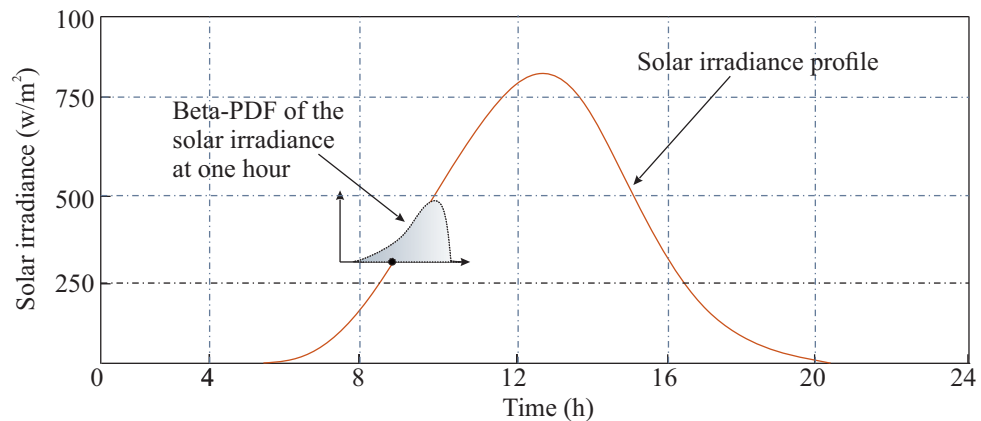


Figure 2. Illustration of solar irradiance in one day.

2.3. Ambient Temperature Uncertainty Model

It was reported in [36] that a normal (Gaussian) PDF is the best parametric distribution to describe the ambient temperature uncertainty, which is given by [37]

$$f_t = \frac{1}{\sigma_T \sqrt{2\pi}} \exp\left(-\frac{(T_a - \mu_T)^2}{2\sigma_T^2}\right), \quad (6)$$

where σ_T and μ_T are the standard deviations and mean value of the hourly ambient temperature T_a , respectively, i.e., its hourly uncertainty is considered in this study.

3. Optimization Problem Formulation

The aim of optimizing an MG size is to find the optimal size of each component in the MG that guarantees the lowest cost of the produced energy from the MG considering the allowable limit of the total loss of power supply (TLPS) considering the uncertainty of the power source within the MG. To achieve that, the following parameters are considered to be optimized: the number of PV modules $N_{pv,m}$, the size of the PV inverter $PV_{inv.size}$, the number of batteries N_{batt} , the number of DGs N_{dg} , and the DG-rated power $P_{r.dg_i}$ where $i \in 1, 2, \dots, N_{dg}$.

According to this, the optimal design problem, which is considered in this study leads to a chance-constrained mixed-integer nonlinear programming (MINLP) problem that can be described in a compact form as follows:

$$\begin{aligned} & \min_{\mathbf{u}} E[LCOE(\mathbf{x}, \mathbf{u}, \boldsymbol{\zeta})] \\ & s.t. \\ & \mathbf{g}(\mathbf{x}, \mathbf{u}, \boldsymbol{\zeta}) = \mathbf{0} \\ & \mathbf{u}_{min} \leq \mathbf{u} \leq \mathbf{u}_{max} \\ & Pr\{TLPS(\mathbf{x}, \mathbf{u}, \boldsymbol{\zeta}) \leq TLPS_{max}\} \geq \alpha_{rel} \\ & \boldsymbol{\zeta} \in \Omega. \end{aligned} \quad (7)$$

where $E[LCOE(\mathbf{x}, \mathbf{u}, \boldsymbol{\zeta})]$ is the mean value of the LCOE, $\mathbf{g}(\mathbf{x}, \mathbf{u}, \boldsymbol{\zeta}) = \mathbf{0}$ is the set of model equations of the MG, \mathbf{x} is the vector of the state variables that comprise the dispatched power from the MG components, \mathbf{u} is the vector of the decision variables, $\boldsymbol{\zeta}$ is the vector of random variables, which includes the solar radiation, ambient temperature, and the blackout starting time and the blackouts period. Since the TLPS value is highly affected by the uncertainty of the power sources in the MG, its limit is formulated as chance-constrained. Therefore, the restriction of the TLPS will be satisfied with a predefined probability level α_{rel} to ensure the reliability of the MG operation.

It is worth mentioning that the studied MGs are considered to be work based on a predefined rule-based operation strategy that gives the PV system the highest priority to cover the load. More information regarding the operation and the models of the studied residential and industrial MGs can be found in [37] and [38], respectively.

3.1. Calculation of LCOE

The levelized cost of energy (LCOE) is the standard criterion for evaluating energy systems investments. In LCOE, the costs of acquiring, owning, operating, and maintaining the energy system over its lifetime are included. The LCOE is calculated by [39]

$$LCOE = \frac{TAPC}{\sum_{t=1}^{T_{max}} P_{disp,t}}, \quad (8)$$

where

$$TAPC = ACC + AMOC + ARC, \quad (9)$$

where T_{max} is equal to 8760 (i.e., the total number of hours in one year), ACC is the annualized capital cost, $AMOC$ is the annualized maintenance and operation cost, and ARC is the annualized replacement cost.

ACC is calculated considering the total capital cost (TCC) and the capital recovery factor (CRF) as follows:

$$ACC = TCC \times CRF, \quad (10)$$

where

$$TCC = CC_{pv} + CC_{b.b} + \sum_{i=1}^{N_{dg}} CC_{dg_i} + CC_{pv.inv} + CC_{b.inv}, \quad (11)$$

where CC_{pv} and $CC_{b.b}$ are the PV array and the battery bank capital cost, respectively. CC_{dg_i} is the i^{th} DG capital cost, $CC_{pv.inv}$, and $CC_{b.inv}$ are the PV inverter and the battery-inverter capital cost, respectively.

In $AMOC$ the maintenance cost of the MG components and the cost of the dispatched power from each power source are considered. Therefore,

$$AMOC = C_{m.pv} + C_{m.b} + C_g + C_{m.dg} + C_{a.op.dg}, \quad (12)$$

where

$$C_g = C_{e.g} \sum_{t=1}^{T_{max}} P_{disp.g}(t), \quad (13)$$

$$C_{a.op.dg}(t) = \sum_{t=1}^{T_{max}} \sum_{i=1}^{N_{dg}} (C_f f_{con.dg_i}(t) + C_{up} \xi_{up.dg_i}(t) + C_d \xi_{d.dg_i}(t)), \quad (14)$$

In Equation (12), $C_{m.pv}$ and $C_{m.b}$ are the annual maintenance costs of the PV array and the battery bank, respectively. C_g is the annual cost of the dispatched energy from the grid-tie line, $C_{m.dg}$, and $C_{a.op.dg}$ are the total annual maintenance and operation costs of the diesel generator set, respectively. In Equation (13), $C_{e.g}$ is the cost of each kWh dispatched from the grid, $P_{disp.g}(t)$ is the total dispatched power from the grid at time t . In Equation (14), C_f is the fuel cost. In $\$/l$, $f_{con.dg_i}(t)$ is the diesel engine fuel consumption, C_{up} and C_d are the startup and shutdown costs, respectively. $\xi_{up.dg_i}(t)$ and $\xi_{d.dg_i}(t)$ are auxiliary binary variables that represent the changes at each diesel generator status.

To calculate ARC , the lifetime of each component is separately estimated at first, then the present worth value (PWV) is used to convert the cost of the component at the replacement time to its present value, and finally, the estimated cost is distributed over the MG lifetime based on CRF . Therefore, the annualized replacement cost is expressed as

$$ARC = CRF \times Comp_{size} \times PWV(N_{rep.x}, lt_x), \quad (15)$$

where $Comp_{size}$ is the component size, $N_{rep.x}$ is the number of replacements of the component during the MG lifetime, and lt_x is the estimated lifetime of it. The lower script x can be the battery bank, the diesel generator, the PV inverter, or the battery inverter. Moreover, PWV is calculated by [26]

$$PWV = \sum_{R=1}^{N_{rep.x}} Comp_{cost} \frac{1}{(1+i)^{R \times lt_x}}, \quad (16)$$

where

$$N_{rep.x} = \left\lceil \frac{lt_{mg}}{lt_x} \right\rceil - 1. \quad (17)$$

The battery lifetime is calculated using the aging model studied in [26]. The lifetime of the PV/battery inverter is assumed to be fixed as 10 years. The diesel generator’s lifetime is defined by the maximum number of hours that can be operated, which is given by the manufacturer. Therefore, the lifetime of the DG will be

$$It_{dg} = \frac{h_{dg.lt}}{h_{op.dg}}, \tag{18}$$

where $h_{dg.lt}$ is the maximum number of operation hours of the DG before reaching the end of its life and $h_{op.dg}$ is the total operation hours of the DG during one year, respectively.

3.2. Optimal Design Constraints

As equality constraints, we use a detailed model to describe the components (i.e., PV array, battery bank, diesel generators, etc.) in the microgrid and an AC model for the power flow description [40,41]. The following inequalities are imposed to satisfy the financial and operational constraints of the design problem

$$0 \leq N_{pv.m} \leq N_{pv.m}^{max} \tag{19a}$$

$$0 \leq PV_{inv.size} \leq PV_{inv.size}^{max} \tag{19b}$$

$$0 \leq N_{batt} \leq N_{batt.max} \tag{19c}$$

$$0 \leq DOD \leq DOD_{max} \tag{19d}$$

$$0 \leq N_{dg} \leq N_{dg.max} \tag{19e}$$

$$0 \leq P_{r.dg_i} \leq P_{r.dg_i}^{max} \quad \forall i = 1, \dots, N_{dg} \tag{19f}$$

$$0 \leq TCC \leq TCC_{max}. \tag{19g}$$

It is to note that the maximum number of the PV modules $N_{pv.m}^{max}$ depends on the area of installation ($A_{pv.inst}$) for the PV array, thus [42]

$$N_{pv.m}^{max} = N_{sg} \times N_{m.sg}, \tag{20}$$

with

$$N_{sg} = \left\lfloor \frac{L_{inst}}{SG_{d.min}} \right\rfloor + 1, \tag{21a}$$

$$N_{m.sg} = \left\lfloor \frac{W_{inst}}{W_{pv.m}} \right\rfloor, \tag{21b}$$

where N_{sg} is number of the PV strings, $N_{m.sg}$ is the maximum number of PV modules per string, L_{inst} is the length of installation area, W_{inst} is the width of installation area, and $W_{pv.m}$ is the width of the PV module. Moreover, $SG_{d.min}$ is the minimum distance between the PV strings (see Figure 3), which is important to prevent the self-shading between the PV strings and is given by the following [43]:

$$SG_{d.min} = PV_{m.l} \times \frac{\sin(\gamma_s + \beta)}{\sin(\gamma_s)}, \tag{22}$$

where $PV_{m.l}$ is the module length (see Figure 3) and γ_s is the angle of the sunlight. A rule of thumb to calculate γ_s is that at noon on December 21 in the northern hemisphere, there must be no shading on the PV strings [43].

In addition to the constraints stated in Equations (19a)–(19g), the following constraint is used to guarantee an acceptable annual loss of power supply $TLPS_{max}$ percentage during the MG operation

$$TLPS(\mathbf{x}, \mathbf{u}, \zeta) \leq TLPS_{max} \tag{23}$$

where $TLPS$ is the annual total loss of power supply that happens when the available power from the MG is not enough to cover the load. Accordingly, the $TLPS$ is calculated by [44]:

$$TLPS = \frac{\sum_{t=1}^{T_{max}} L_p(t)}{T_{max}} \times 100, \quad (24)$$

where $L_p(t)$ is a binary variable, i.e., $L_p(t) = 1$ when the available power from the MG is lower than the required load, else $L_p(t) = 0$.

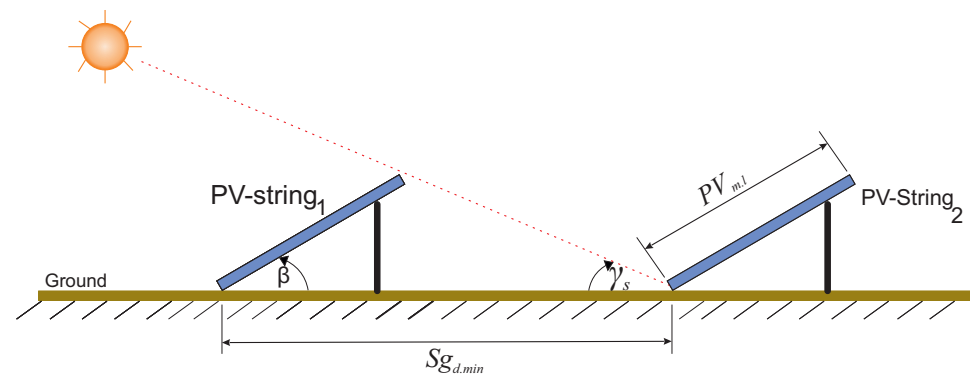


Figure 3. Illustration of a PV array installation.

Since the $TLPS$ value is affected by the uncertainty of the considered random parameters, it will be uncertain to satisfy Equation (23). Therefore, this constraint is formulated as a chance constraint, as indicated in Equation (7).

4. Solution Method

In general, there are two main approaches to solving nonlinear CCOPT problems, namely, the analytic approximation and the numerical approximation approaches [45]. In this study, the formulated optimization problem is a chance-constrained MINLP problem that cannot be solved using the available analytic approximation methods. The solution of the problem by a numerical approximation method requires the evaluation of the probability of the chance constraint and the expected value of the objective function by a set of samples extracted from the PDF of the uncertain parameters [46].

Therefore, a simulation-based solution framework is used in this study, as shown in Figure 4. In each iteration, the battery lifetime is calculated using the mean values of the uncertain input parameters based on the battery aging model in [26]. Then, the Monte Carlo simulation is used to calculate the $TLPS$ and $LCOE$ values for each extracted sample from the PDF of the uncertain parameters. After that, an approximated solution for the chance constraint (see Equation (7)) is calculated by

$$Pr\{TLPS(\mathbf{x}, \mathbf{u}, \zeta) \leq TLPS_{max}\} = \frac{\text{Number of feasible samples}}{\text{Total number of the samples}}, \quad (25)$$

where the feasible samples are those lower than $TLPS_{max}$. Finally, the expected value of the $LCOE$ is calculated and evaluated by the optimizer. The procedure is repeated until the stopping criteria of the optimizer are satisfied. In this study, a genetic algorithm (GA) is used as the optimizer because of its ability to solve complex optimization problems irrespective of the model of the system [47].

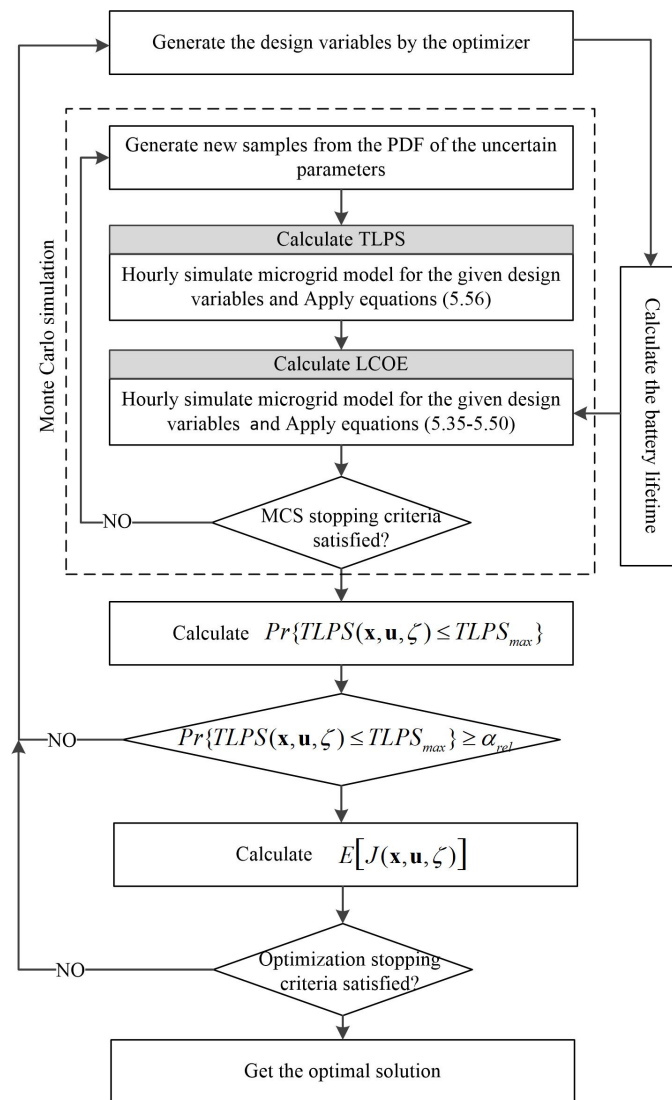


Figure 4. Flowchart of the stochastic simulation-based optimization.

5. Case Studies

The proposed design approach is applied to optimize a residential PV battery MG and an industrial PV–battery–diesel MGs studied in [26] and [48], respectively. Solar irradiance data [49] and grid blackout historical data are from Gaza city in Palestine (latitude = 31.42° and longitude = 34.38°). The parameters of the battery cell are taken from [26]. The parameters in the economic model are listed in Table 1. Moreover, the MG components' capital cost, maintenance cost percentage from the capital cost, and lifetime are shown in Table 2.

Table 1. Economic model parameters of MG design [40,50].

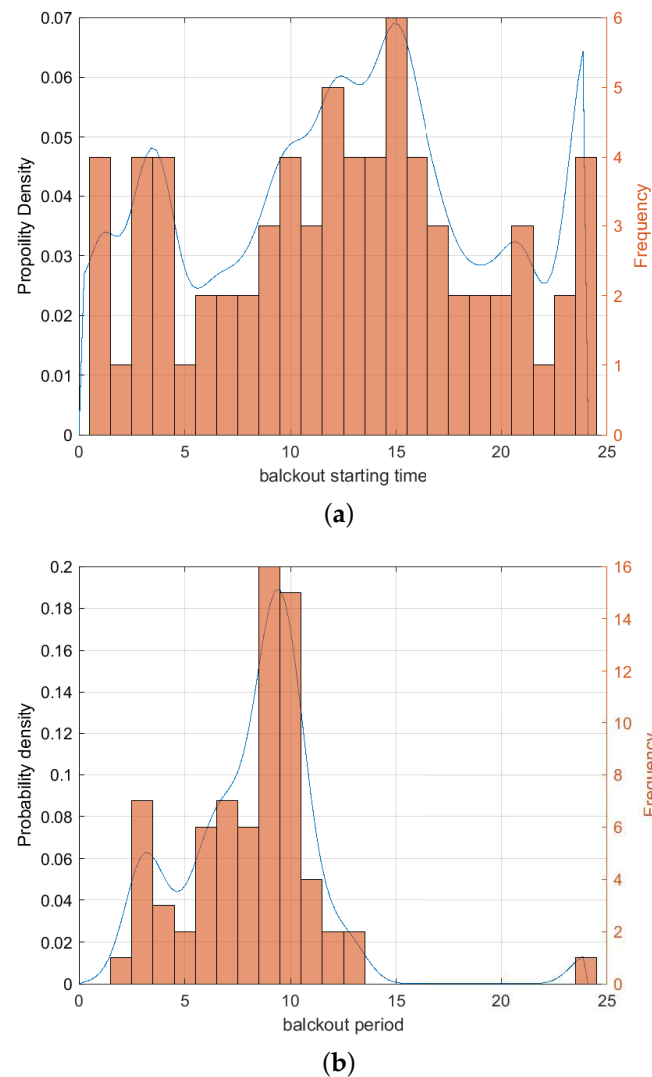
Parameter	r'_i (-)	r_f (-)	C_f (\$/l)	C_g (\$/kWh)	l_t (Years)
Value	6.89%	3.16%	1.3%	0.15%	20

Using KDE, the PDF of the starting time and the period of the grid blackout is shown in Figure 5. The confidence level in the chance constraint is chosen to be 98%.

All the computation is carried out on a Linux server with 64 processors of type AMD-Epyc7601 X86-64 using the MATLAB 2018b software.

Table 2. Microgrid components' capital cost, maintenance cost, and lifetime.

Parameter	CC	MC	Lifetime
PV array	550 \$/kW _p	0.5%	20 (years)
PV inverter	300 \$/kW	0.5%	10 (years)
Battery bank	150 \$/kWh	1%	to be calculated
Battery inverter	300 \$/kW	0.5%	10 (years)
Diesel Generator	250 \$/kW	8%	10,000 (h)

**Figure 5.** Uncertainty of grid blackout. (a) Histogram of the blackout starting times (orange bars) and the fitted PDF (blue line). (b) Histogram of the blackout periods (orange bars) and the fitted PDF (blue line).

5.1. Optimal Design of a Residential MG

In this case study, the decision variables include only the PV array and the battery bank size as well as the *DOD* value of the battery bank. The residential loads for four seasonal days in workdays and weekends are taken from [26] with a 5 kW peak value. Moreover, the maximum value of *TCC* is considered to be 3500\$. The maximum *TLPS_{max}* is selected to be 2% with a reliability level of 98%.

To illustrate the impact of considering the parameter uncertainties, both the deterministic and stochastic optimal design of the residential MG are performed. In the deterministic case, the mean values of the solar irradiance and the ambient temperature in each season are used to build yearly input data. The mean values for the starting time and the period of

daily grid blackouts are used, respectively, in the problem formulation. In the stochastic case, the chance-constrained optimization under the uncertainties proposed in this paper is used to solve the design problem.

The resulting optimal battery bank and the PV array sizes, as well as the *DOD* optimal value, for both scenarios, are given in Table 3. It can be noticed from the table that the size of the battery bank and the PV array, as well as the *DOD* value, are larger in the stochastic case. Moreover, the realized reliability level of the chance constraint is calculated for both cases via the Monte Carlo simulation. It can be seen that neglecting the parameter uncertainties will lead to a considerable detriment in the reliability of the MG.

Table 3. Optimal design results of the residential MG.

Parameter	N_{batt} (-)	$N_{pv,m}$ (-)	<i>DOD</i> (-)	<i>LCOE</i> (\$/kWh)	α_{rel} (%)
Deterministic	8	10	0.56	0.1835	27.8
Stochastic	10	12	0.68	0.2059	98

5.2. Optimal Design of an Industrial MG

The optimal design of a PV–battery–diesel MG under uncertainty is carried out here. The active power load profiles are taken from [48] with a peak value of 500 kW.

Moreover, the maximum value of the *TCC* is assumed to be 720,000\$.

It was shown in [38] that a power deficit in industrial facilities is very expensive. Therefore, in this case study, the maximum $TLPS_{max}$ is selected to be 0% (i.e., there should be no loss of power supply at any time) with a reliability level of 98%.

To show the importance of considering the parameter uncertainties, the optimal design problem is solved by considering the following different scenarios:

- Scenario 1: deterministic optimization employing the mean values of grid blackout starting time and duration, solar irradiance, and ambient temperature;
- Scenario 2: stochastic optimization considering the uncertainty of grid blackout starting time and duration, solar irradiance, and ambient temperature;
- Scenario 3: as in Scenario 1, but assume the blackout starts at midnight to include the daily low load period in the grid blackout duration.

The results of solving these three problems are given in Table 4. It can be seen that there is no significant difference in the sizes of the components in Scenario 1 and Scenario 2. Moreover, it can be noticed that the total rated capacity of the DGs in both scenarios is equal to the maximum load value (i.e., 500 kW), which makes the MG able to cover the load at any time (i.e., $TLPS = 0$). Nonetheless, the difference in DGs sizes is due to the difference in load levels to be covered by the DGs. Moreover, there is a notable difference in the *LCOE* values in Scenario 1 and Scenario 2, although the component sizes are nearly equal. Thus, if the uncertainties of the input parameters are not considered, there will be a wrong estimation for the output energy cost over the MG's lifetime, which could lead to wrong investment decisions.

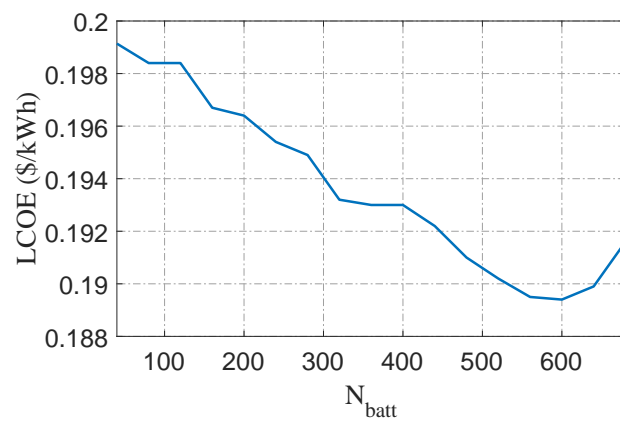
A lower *LCOE* value can be achieved in Scenario 1 and Scenario 2 if the *TCC* constraint is neglected. As an example, the effect of increasing the battery number is shown in Figure 6, it can be seen that a lower *LCOE* can be reached with 600 and 760 batteries in scenarios 1 and 2, respectively. This means that a bigger size of the battery bank is required to decrease the *LCOE*, considering parameter uncertainties.

In Scenario 3, the blackout duration is shifted to a low load duration (from 0 to 8 o'clock). As shown in Table 4, the resulting total rated capacity of the DGs is equal to the maximum load value in the specified period (i.e., 420 kW) to cover the load at any time during the blackout duration (i.e., $TLPS = 0$). However, the optimal solution of this scenario leads to a very low reliability level. This is because the MG is unable to cover a load higher than the size of the DG in the event of a grid blackout in periods other than the specified period. Therefore,

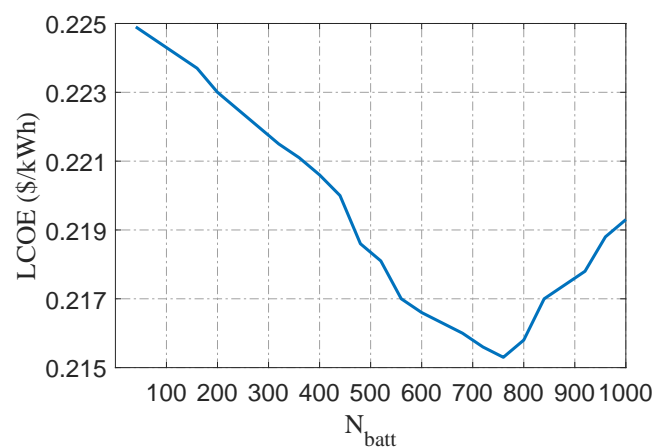
it is highly essential to consider the grid blackout uncertainty so as to ensure covering the load at any time of the year.

Table 4. Optimal design results of the Industrial MG.

Parameter	Scenario 1	Scenario 2	Scenario 3
PV array	1450	1450	1450
PV inverter (Kw)	280	280	280
Battery size	568	568	464
DOD (%)	76	73	65
Diesel number	3	3	3
Diesel generator (Kw)	60	80	70
Diesel generator (Kw)	120	170	130
Diesel generator (Kw)	270	250	220
Battery life (year)	3.03	3.17	3.58
LCOE (\$/Kw)	0.1896	0.2169	0.1729
$TLPS_{max}$ (%)	0%	0%	0%
α_{rel} (%)	100%	100%	16.61%



(a)



(b)

Figure 6. Impact of the number of batteries on the design problem. (a) The relation between the number of batteries and the $LCOE$ in Scenario 1. (b) The relation between the number of batteries and the $LCOE$ in Scenario 2.

The annual cost analysis of the MG (in Scenario 1) is illustrated in Figure 7. It can be seen that the cost of the dispatched power from the grid and the DG operation as well as

maintenance costs $C_{o\&m.dg}$ are substantial. Based on the following operation strategy, these costs can be reduced by increasing the PV system and the battery bank capacities. Therefore, the maximum number of PV modules is found by the optimizer as the optimal solution. In addition, increasing the number of batteries decreases the operation and maintenance cost (as shown in Figure 8); however, when the decrease in the DG operation cost cannot compensate for the increment in ACC, ARC, and battery charging costs (see, the dashed black line in Figure 8), then LCOE starts to rise, as shown in Figure 6.

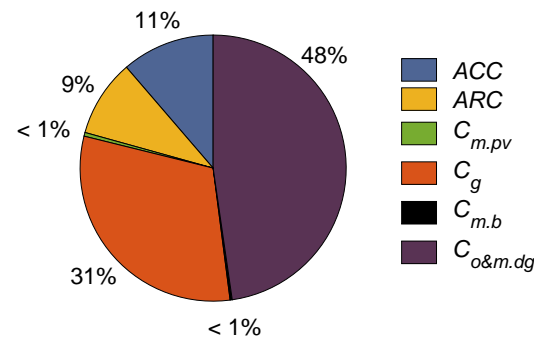


Figure 7. The annual cost analysis of the PV–battery–diesel MG.

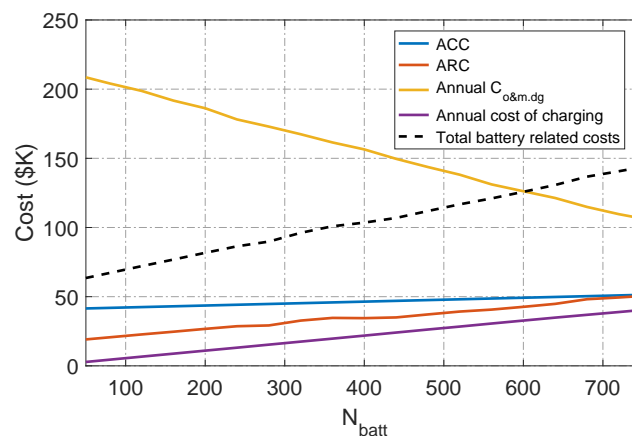


Figure 8. Analyze the effect of increasing the battery number on the annual costs.

6. Conclusions

A chance-constrained optimal design approach for PV-based MG is proposed in this paper to increase the reliability of supplying energy under uncertainty. The uncertain blackout starting time and duration are modeled by non-parametric PDFs, and the uncertain solar irradiance and ambient temperature with parametric PDFs, respectively. The restriction of the annual total loss of the power supply ($TLPS$) is treated as a chance constraint. A simulation-based optimization approach is used to solve the chance-constrained MINLP problem. The proposed approach is able to optimize the sizes of MG's components; meanwhile, the levelized cost of energy is minimized, and the specified $TLPS$ is satisfied. The results of the two case studies show that it is important to consider the uncertainties that have a considerable effect on the reliability of the optimal design.

Author Contributions: Conceptualization, M.A. and P.L.; methodology, P.L.; software, M.A.; validation, M.A.; formal analysis, M.A.; investigation, M.A.; resources, M.A.; data curation, M.A.; writing—original draft preparation, M.A. and P.L.; writing—review and editing, P.L.; visualization, M.A.; supervision, P.L.; project administration, M.A. and P.L.; funding acquisition, P.L. All authors have read and agreed to the published version of the manuscript.

Funding: This work was supported by the German Academic Exchange Service (DAAD).

Data Availability Statement: The data presented in this study are available on request from the corresponding author. The data are not publicly available due to privacy.

Conflicts of Interest: The authors declare no conflict of interest. The funders had no role in the design of the study; in the collection, analyses, or interpretation of data; in the writing of the manuscript; or in the decision to publish the results.

References

1. Aien, M.; Hajebrahimi, A.; Fotuhi-Firuzabad, M. A comprehensive review on uncertainty modeling techniques in power system studies. *Renew. Sustain. Energy Rev.* **2016**, *57*, 1077–1089. [[CrossRef](#)]
2. Zakaria, A.; Ismail, F.B.; Lipu, M.H.; Hannan, M. Uncertainty models for stochastic optimization in renewable energy applications. *Renew. Energy* **2020**, *145*, 1543–1571. [[CrossRef](#)]
3. Kamjoo, A.; Maheri, A.; Putrus, G.A. Chance constrained programming using non-Gaussian joint distribution function in design of standalone hybrid renewable energy systems. *Energy* **2014**, *66*, 677–688. [[CrossRef](#)]
4. Maleki, A.; Khajeh, M.G.; Ameri, M. Optimal sizing of a grid independent hybrid renewable energy system incorporating resource uncertainty, and load uncertainty. *Int. J. Electr. Power Energy Syst.* **2016**, *83*, 514–524. [[CrossRef](#)]
5. Bashir, M.; Sadeh, J. Optimal sizing of hybrid wind/photovoltaic/battery considering the uncertainty of wind and photovoltaic power using Monte Carlo. In Proceedings of the 2012 11th International Conference on Environment and Electrical Engineering, Venice, Italy, 18–25 May 2012; IEEE: Piscataway, NJ, USA, 2012; pp. 1081–1086.
6. Arun, P.; Banerjee, R.; Bandyopadhyay, S. Optimum sizing of photovoltaic battery systems incorporating uncertainty through design space approach. *Sol. Energy* **2009**, *83*, 1013–1025. [[CrossRef](#)]
7. Roy, A.; Kedare, S.B.; Bandyopadhyay, S. Optimum sizing of wind-battery systems incorporating resource uncertainty. *Appl. Energy* **2010**, *87*, 2712–2727. [[CrossRef](#)]
8. Kamjoo, A.; Maheri, A.; Dizqah, A.M.; Putrus, G.A. Multi-objective design under uncertainties of hybrid renewable energy system using NSGA-II and chance constrained programming. *Int. J. Electr. Power Energy Syst.* **2016**, *74*, 187–194. [[CrossRef](#)]
9. Yang, D.; Jiang, C.; Cai, G.; Huang, N. Optimal sizing of a wind/solar/battery/diesel hybrid microgrid based on typical scenarios considering meteorological variability. *IET Renew. Power Gener.* **2019**, *13*, 1446–1455. [[CrossRef](#)]
10. Dong, J.; Gao, F.; Guan, X.; Zhai, Q.; Wu, J. Storage-reserve sizing with qualified reliability for connected high renewable penetration micro-grid. *IEEE Trans. Sustain. Energy* **2016**, *7*, 732–743. [[CrossRef](#)]
11. Nguyen-Hong, N.; Nguyen-Duc, H. Optimal sizing of energy storage devices in wind-diesel systems considering load growth uncertainty. In Proceedings of the 2016 IEEE International Conference on Sustainable Energy Technologies (ICSET), Hanoi, Vietnam, 14–17 November 2016; IEEE: Piscataway, NJ, USA, 2016; pp. 54–59.
12. Xia, S.; Chan, K.; Luo, X.; Bu, S.; Ding, Z.; Zhou, B. Optimal sizing of energy storage system and its cost-benefit analysis for power grid planning with intermittent wind generation. *Renew. Energy* **2018**, *122*, 472–486. [[CrossRef](#)]
13. Abdulgalil, M.A.; Khalid, M.; Alismail, F. Optimal Sizing of Battery Energy Storage for a Grid-Connected Microgrid Subjected to Wind Uncertainties. *Energies* **2019**, *12*, 2412. [[CrossRef](#)]
14. Zhang, H.; Li, P. Chance Constrained Programming for Optimal Power Flow Under Uncertainty. *IEEE Trans. Power Syst.* **2011**, *26*, 2417–2424. [[CrossRef](#)]
15. Zhang, H.; Li, P. Application of sparse-grid technique to chance constrained optimal power flow. *IET Gener. Transm. Distrib.* **2013**, *7*, 491–499. [[CrossRef](#)]
16. Khoury, J.; Mbayed, R.; Salloum, G.; Monmasson, E. Optimal sizing of a residential PV-battery backup for an intermittent primary energy source under realistic constraints. *Energy Build.* **2015**, *105*, 206–216. [[CrossRef](#)]
17. Hijo, M.; Felgner, F.; Frey, G. Energy Management Scheme for Buildings Subject to Planned Grid Outages. *J. Eng. Res. Technol.* **2016**, *3*, 58–65.
18. Nayar, C.V.; Ashari, M.; Keerthipala, W. A grid-interactive photovoltaic uninterruptible power supply system using battery storage and a back up diesel generator. *IEEE Trans. Energy Convers.* **2000**, *15*, 348–353. [[CrossRef](#)]
19. Ndwali, P.K.; Njiri, J.G.; Wanjiru, E.M. Optimal Operation Control of Microgrid Connected Photovoltaic-Diesel Generator Backup System Under Time of Use Tariff. *J. Control. Autom. Electr. Syst.* **2020**, *31*, 1001–1014. [[CrossRef](#)]
20. Falama, R.Z.; Kaoutoing, M.D.; Mbakop, F.K.; Dumbava, V.; Makloufi, S.; Djongyang, N.; Salah, C.B.; Doka, S.Y. A comparative study based on a techno-environmental-economic analysis of some hybrid grid-connected systems operating under electricity blackouts: A case study in Cameroon. *Energy Convers. Manag.* **2022**, *251*, 114935. [[CrossRef](#)]
21. Zhang, T.; Cialdea, S.; Orr, J.A.; Emanuel, A.E. Outage Avoidance and Amelioration Using Battery Energy Storage Systems. *IEEE Trans. Ind. Appl.* **2016**, *52*, 5–10. [[CrossRef](#)]
22. Esmaeilian, A.; Kezunovic, M. Prevention of Power Grid Blackouts Using Intentional Islanding Scheme. *IEEE Trans. Ind. Appl.* **2017**, *53*, 622–629. [[CrossRef](#)]
23. Dong, J.; Zhu, L.; Su, Y.; Ma, Y.; Liu, Y.; Wang, F.; Tolbert, L.M.; Glass, J.; Bruce, L. Battery and backup generator sizing for a resilient microgrid under stochastic extreme events. *IET Gener. Transm. Distrib.* **2018**, *12*, 4443–4450. [[CrossRef](#)]
24. Zhou, J.; Tsiannikas, S.; Birnie, D.P., III; Coit, D.W. Economic and resilience benefit analysis of incorporating battery storage to photovoltaic array generation. *Renew. Energy* **2019**, *135*, 652–662. [[CrossRef](#)]

25. Tsianikas, S.; Zhou, J.; Birnie, D.P., III; Coit, D.W. Economic trends and comparisons for optimizing grid-outage resilient photovoltaic and battery systems. *Appl. Energy* **2019**, *256*, 113892. [[CrossRef](#)]
26. Alramlawi, M.; Li, P. Design Optimization of a Residential PV-Battery Microgrid with a Detailed Battery Lifetime Estimation Model. *IEEE Trans. Ind. Appl.* **2020**, *56*, 2020–2030. [[CrossRef](#)]
27. Soize, C. Stochastic modeling of uncertainties in computational structural dynamics—Recent theoretical advances. *J. Sound Vib.* **2013**, *332*, 2379–2395. [[CrossRef](#)]
28. Chen, Y.C. A tutorial on kernel density estimation and recent advances. *Biostat. Epidemiol.* **2017**, *1*, 161–187. [[CrossRef](#)]
29. Bowman, A.W.; Azzalini, A. *Applied Smoothing Techniques for Data Analysis: The Kernel Approach with S-Plus Illustrations*; OUP Oxford: Oxford, UK, 1997; Volume 18.
30. Voskrebenezv, A.; Riechelmann, S.; Bais, A.; Slaper, H.; Seckmeyer, G. Estimating probability distributions of solar irradiance. *Theor. Appl. Climatol.* **2015**, *119*, 465–479. [[CrossRef](#)]
31. MATLAB. *Statistics Toolbox User's Guide*; The MathWorks Inc.: Natick, MA, USA, 2004.
32. The Humanitarian Impact of Gaza's Electricity and Fuel Crisis. 2015. Available online: <https://www.un.org/unispal/document/auto-insert-204698/> (accessed on 28 February 2024).
33. Mavromatidis, G.; Orehounig, K.; Carmeliet, J. Uncertainty and global sensitivity analysis for the optimal design of distributed energy systems. *Appl. Energy* **2018**, *214*, 219–238. [[CrossRef](#)]
34. Mena, R.; Hennebel, M.; Li, Y.F.; Ruiz, C.; Zio, E. A risk-based simulation and multi-objective optimization framework for the integration of distributed renewable generation and storage. *Renew. Sustain. Energy Rev.* **2014**, *37*, 778–793. [[CrossRef](#)]
35. Chia, E.; Hutchinson, M. The beta distribution as a probability model for daily cloud duration. *Agric. For. Meteorol.* **1991**, *56*, 195–208. [[CrossRef](#)]
36. Prusty, B.R.; Jena, D. A sensitivity matrix-based temperature-augmented probabilistic load flow study. *IEEE Trans. Ind. Appl.* **2017**, *53*, 2506–2516. [[CrossRef](#)]
37. Nikmehr, N.; Ravadanegh, S.N. Optimal power dispatch of multi-microgrids at future smart distribution grids. *IEEE Trans. Smart Grid* **2015**, *6*, 1648–1657. [[CrossRef](#)]
38. Wacker, G.; Billinton, R. Customer cost of electric service interruptions. *Proc. IEEE* **1989**, *77*, 919–930. [[CrossRef](#)]
39. Tezer, T.; Yaman, R.; Yaman, G. Evaluation of approaches used for optimization of stand-alone hybrid renewable energy systems. *Renew. Sustain. Energy Rev.* **2017**, *73*, 840–853. [[CrossRef](#)]
40. Alramlawi, M.; Gabash, A.; Mohagheghi, E.; Li, P. Optimal operation of hybrid PV-battery system considering grid scheduled blackouts and battery lifetime. *Sol. Energy* **2018**, *161*, 125–137. [[CrossRef](#)]
41. Alramlawi, M.; Mohagheghi, E.; Li, P. Predictive active-reactive optimal power dispatch in PV-battery-diesel microgrid considering reactive power and battery lifetime costs. *Sol. Energy* **2019**, *193*, 529–544. [[CrossRef](#)]
42. Castellano, N.N.; Parra, J.A.G.; Valls-Guirado, J.; Manzano-Agugliaro, F. Optimal displacement of photovoltaic array's rows using a novel shading model. *Appl. Energy* **2015**, *144*, 1–9. [[CrossRef](#)]
43. Mertens, K. *Photovoltaics: Fundamentals, Technology, and Practice*; John Wiley & Sons: Hoboken, NJ, USA, 2018.
44. Yang, H.; Wei, Z.; Chengzhi, L. Optimal design and techno-economic analysis of a hybrid solar-wind power generation system. *Appl. Energy* **2009**, *86*, 163–169. [[CrossRef](#)]
45. Geletu, A.; Klöppel, M.; Zhang, H.; Li, P. Advances and applications of chance-constrained approaches to systems optimisation under uncertainty. *Int. J. Syst. Sci.* **2012**, *44*, 1209–1232. [[CrossRef](#)]
46. Diwekar, U.M.; Kalagnanam, J.R. Efficient sampling technique for optimization under uncertainty. *AIChE J.* **1997**, *43*, 440–447. [[CrossRef](#)]
47. Stojanovski, G.; Stankovski, M. *Model Predictive Controller Employing Genetic Algorithm Optimization of Thermal Processes with Non-Convex Constraints*; INTECH Open Access Publisher: London, UK, 2012.
48. Alramlawi, M.; Gabash, A.; Mohagheghi, E.; Li, P. Optimal Operation of PV-Battery-Diesel MicroGrid for Industrial Loads Under Grid Blackouts. In Proceedings of the 2018 IEEE International Conference on Environment and Electrical Engineering and 2018 IEEE Industrial and Commercial Power Systems Europe (EEEIC/I CPS Europe), Palermo, Italy, 12–15 June 2018; IEEE: Piscataway, NJ, USA, 2018; pp. 1–5.
49. Solar Energy Services for Professionals. Available online: <http://www.soda-pro.com> (accessed on 28 February 2024).
50. Trading Economics. Available online: <http://www.tradingeconomics.com> (accessed on 28 February 2024).

Disclaimer/Publisher's Note: The statements, opinions and data contained in all publications are solely those of the individual author(s) and contributor(s) and not of MDPI and/or the editor(s). MDPI and/or the editor(s) disclaim responsibility for any injury to people or property resulting from any ideas, methods, instructions or products referred to in the content.